Journal of Power Sources 206 (2012) 144–152

Contents lists available at SciVerse ScienceDirect

Journal of Power Sources

journal homepage: www.elsevier.com/locate/jpowsour

Innovative model-based control approach of a proton exchange membrane fuel cell system

C. Damour[a], D. Grondin[a], M. Benne[a], B. Grondin-Perez[a], J. Deseure[b,*], J.P. Chabriat[a]

[a] Laboratoire d'Energétique, d'Electronique et Procédés (LE2P), University of La Réunion, 15 Av. René Cassin, BP 7151, 97715 Saint-Denis, France
[b] Laboratoire d'Électrochimie et de Physico chimie des Matériaux et des Interfaces (LEPMI), UMR 5279 CNRS/Grenoble-INP/UJF/UdS, Phelma/Grenoble-INP, 1130 rue de la Piscine, Domaine Universitaire, BP 75, 38402 Saint-Martin d'Hères Cedex, France

ARTICLE INFO

Article history:
Received 1 December 2011
Received in revised form 11 January 2012
Accepted 13 January 2012
Available online 7 February 2012

Keywords:
Proton exchange membrane fuel cell
Model-based control
Predictive control
Linearizing control

ABSTRACT

This work highlights the gains of an innovative model-based control approach applied to a proton exchange membrane fuel cell (PEMFC) system, included in a stand-alone hybrid generator. This approach proposes a multivariable setpoint tracking of the PEMFC output power and temperature. The freshness of this approach is based on the combination of a nonlinear model-based predictive control strategy (NMPC) and a global linearizing control (GLC) algorithm.

The performance of the proposed control strategy is confirmed thanks to simulations of varying control scenarios. Results show good performance in setpoint tracking, disturbances rejection and robustness against plant/model mismatch in presence of noisy signals. Moreover, for similar setpoint point tracking accuracy, the proposed control strategy appears to be four times faster than a classical multivariable NMPC strategy. According to real-time application objectives, this control strategy appears as a promising option to be implanted in the overall control scheme of the stand-alone hybrid power generator.

1. Introduction

Nowadays, in a context of sustainable development, and to deal with the serious problem of global warming, renewable energy sources such as solar, wind or biomass resources represent a promising alternative to the traditional fossil fuels. In a general point of view subtropical region, solar radiation is high, which is favorable for various kinds of solar energy implementations. In particular case of the tropical islands photovoltaic appears as one best strategy in their energy mix. Indeed, photovoltaic (PV) technology directly converts solar energy into electricity, without greenhouse gases and air pollutant emissions. Nevertheless, this technology has two main drawbacks: its low efficiency and the nature of solar power, intermittent and unreliable. In practice, considering the zero cost of solar energy, the weak conversion rate is usually not considered as a major disadvantage. However, PV power conversion is limited to daylight period and strongly influenced by the weather.

To overcome these limitations, one of the most widespread methods is to integrate PV generators with other power sources such as fuel cells, batteries backup or diesel generators [1,2]. Due to its high efficiency, fast power response, high power density and low operating temperature, the proton exchange membrane fuel cell (PEMFC) appears as a suitable and reliable option to be combined with photovoltaic arrays. Recent studies showed its great potential to solve the inherent problem of intermittent power generation of PV arrays [3–5]. Regarding photovoltaic-fuel cell (PVFC) hybrid systems, the main part of the process control remains the control of the fuel cell.

A fuel cell is a nonlinear and strongly coupled dynamic system. It is a multi-input multi-output (MIMO) system based on multiphase flow, electrochemical reactions and heat transfer. Since few years, many control strategies have been developed to control PEMFC and SOFC (solid oxide fuel cell) systems, based on various control algorithms, manipulated and controlled variables. Huang et al. [6] designed a fuzzy PID controller to regulate hydrogen flow rate, resulting in an optimization of the hydrogen consumption. Wang and Ko [7] proposed a multivariable robust PID controller, based on a classical PID approach combined to the merits of robust control, to regulate air and hydrogen flow rates. Results obtained showed good performance in terms of stability and efficiency using a simple control structure. Methekar et al. [8] considered a MIMO system and proposed two PID control strategies. Using a steady-state relative gain array (RGA) analysis, these authors showed that hydrogen and coolant inlet flow rates are suitable manipulated variables to control the output power and temperature of a PEMFC, respectively. Zhang et al. [9] proposed a nonlinear predictive control approach to control output power, fuel utilization and temperature of a SOFC using the current density, the fuel and air flow rates are used as

* Corresponding author. Tel.: +33 476826586; fax: +33 476826777.
E-mail address: jonathan.deseure@lepmi.grenoble-inp.fr (J. Deseure).

0378-7753/$ – see front matter © 2012 Elsevier B.V. All rights reserved.
doi:10.1016/j.jpowsour.2012.01.096

Nomenclature

A_{fc}	cell electrode area, cm^2
C_{dl}	double layer capacitance of single cell, F
C_{H_2}	hydrogen concentration at the anode/membrane interface, mol cm^{-3}
C_{O_2}	oxygen concentration at the cathode/membrane interface, mol cm^{-3}
C_{pw}	water heat capacity, J kg^{-1} K^{-1}
C_t	thermal capacitance, J K^{-1}
$\dot{E}_{cool}$	heat flux removed by the heat exchanger, W
$\dot{E}_{elec}$	power consumption by the electrical load, W
$\dot{E}_{loos}$	heat flux dissipated to the surroundings, W
E_{Nernst}	thermodynamic potential, V
$\dot{E}_{tot}$	total power delivered by the stack, W
F	Faraday constant, 96485 C mol^{-1}
h_{amb}	convective heat transfer coefficient, W m^{-2} K^{-1}
h_{cond}	heat exchanger conduction index, W K^{-1}
h_{conv}	heat exchanger convection index, W K^{-1} A^{-1}
I	cell/stack current, A
J	cost function of regulator
$k_0,\ldots,k_{r-1}$	controller tuning parameter
$L_f^r h$	rth Lie derivatives of $h(x(t))$ along f
$L_g^r h$	rth Lie derivatives of $h(x(t))$ along g.
l_m	membrane thickness, cm
$\dot{m}_{cw}$	cooling water mass flow rate, kg s^{-1}
$\dot{m}_{H_2,in}$	hydrogen inlet flow rate, mol s^{-1}
$\dot{m}_{H_2,out}$	hydrogen outlet flow rate, mol s^{-1}
$\dot{m}_{H_2,reacted}$	rate of hydrogen consumption, mol s^{-1}
$\dot{m}_{O_2,in}$	oxygen inlet flow rate, mol s^{-1}
$\dot{m}_{O_2,out}$	oxygen outlet flow rate, mol s^{-1}
$\dot{m}_{O_2,reacted}$	rate of oxygen consumption, mol s^{-1}
N_{cell}	number of cells
N_u	control horizon, s
N_y	predictive horizon, s
N_1	optimization parameter
P_{H_2}	hydrogen partial pressure, atm
$P_{H_2}^{in}$	hydrogen partial pressure at the inlet, atm
P_{O_2}	oxygen partial pressure, atm
$P_{O_2}^{out}$	oxygen partial pressure at the outlet, atm
r	relative degree of the system
R	universal gas constant, 8.314 J mol^{-1} K^{-1}
R_{act}	activation resistance, Ω
S	external stack surface, m^2
t	time, s
T	stack temperature, K
T_{amb}	ambient temperature, K
$T_{c,in}$	cooling water inlet temperature, K
$T_{c,out}$	cooling water outlet temperature, K
u	input vector
$u(k)$	control variable at time k
U_a	overall heat transfer coefficient
V_{an}	anode volume, m^3
V_{act}	absolute value of activation overvoltage, V
V_{ca}	cathode volume, m^3
V_{cell}	single cell voltage, V
V_{stack}	stack voltage, V
V_w	cooling water volume, m^3
w	setpoint
x	state vector
y	output vector
y_m	model output
y_{sp}	setpoint to track
y_{sr}	target value

Greek letters

α	filtering parameter
α_0	controller tuning parameter
β	weighting parameter
ΔH	hydrogen consumption enthalpy, kJ mol^{-1}
γ	weighting parameter
η_{act}	activation overvoltage, V
η_{ohm}	ohmic overvoltage, V
ρ_w	water density, kg m^{-3}
$\xi_1,\ldots,\xi_4$	activation overvoltage parametric coefficients, V or V K^{-1}

manipulated variables. In this approach, the exit gases composition and temperature are estimated using moving horizon estimation (MHE) methods. Wu et al. [10] designed a multi-loop nonlinear predictive control scheme to regulate stack temperature and oxygen excess ratio of a hybrid energy system (wind turbine and PEMFC) by manipulating coolant and air mass flow rates. Even if the simulation results are encouraging, the authors underline that some devices and design are not taken into account (e.g. hydrogen storage, power management and inverters). Li et al. [11] proposed a nonlinear robust control of a PEMFC based on a state feedback linearizing approach. This well-known nonlinear approach allows to obtain a nonlinear control law directly from the dynamic nonlinear model of the process. To improve the robustness of the system, the authors proposed to add a H_∞ robust control strategy to the state feedback control law.

This study focuses on the control of a 5 kW PEMFC, included in a stand-alone hybrid renewable power generation system designed for a typical household in La Reunion Island located at following geographic coordinate (21° 6′ S/55° 36′ E). In this purpose, a MIMO dynamic nonlinear model of the PEMFC, dedicated to nonlinear model-based control approaches, is proposed. Directly based on the nonlinear dynamic model of the system, a nonlinear model-based predictive control strategy (NMPC) and a global linearizing control (GLC) approach are proposed to control the output power and the temperature of the PEMFC, respectively. This original control scheme, designed for on-line applications, appears to be suitable to cope with large setpoint changes, severe unmeasured disturbances and plant/model mismatch.

The subsequent developments of the manuscript are organized as follows: Section 2 is dedicated to the description of the system and the model design. The third section deals with the control design, and details the NMPC of the output power and the GLC of the temperature of the stack. In Section 4, the performance of the proposed control strategy, in terms of setpoint tracking, disturbances rejection and robustness against plant/model mismatch, is demonstrated via simulation. Finally, conclusions and prospects are drawn in Section 5.

2. System design and modeling

2.1. System description

This work deals with the modeling and control of a Ballard 5 kW PEMFC, represented in Fig. 1.

This PEMFC is including in a stand-alone hybrid system. This hybrid generator comprises a PV array, an electrolyzer, a hydrogen tank and a PEMFC. The PV array is designed to satisfy the power demand of a typical household in La Reunion. In the absence of sufficient solar radiation, the PEMFC is designed to compensate for the PV generator, assuming the hydrogen storage problem solved. During the daylight period, the solar power is converted into

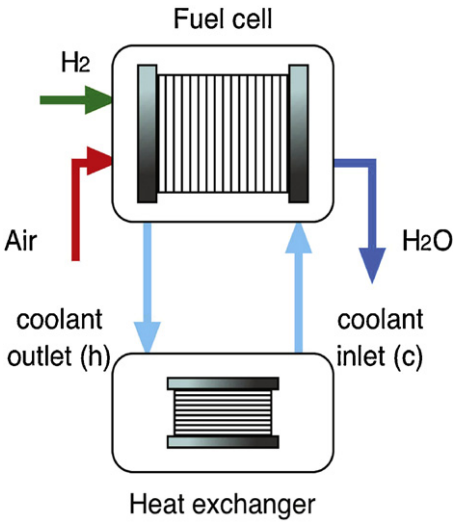

Fig. 1. Scheme of the PEMFC system (with heat exchanger system).

electric power. A fraction of PV power is used to reach the power demand of user load whereas excess energy is stored in hydrogen via electrolysis. The fuel cell generator can be used both at night to cover the energy demand, and during day as backup generator when solar power is deficient (e.g. during a period of low solar radiation). Fig. 2 illustrates a typical daily power consumption of a household located in La Reunion Island, and the power delivered by the PV array. Energy conversion via electrolysis and fuel cell has an efficiency of 30–35% [12]. Considering an estimated household electricity consumption of 112 Wh m^{-2} day^{-1} and using polycrystalline PV cells with an efficiency of 12.4%, a 40 m^2 surface of PV array is considered to deliver the needed power.

From midnight to dawn (0:00–6:30), the fuel cell is used to cover the power demand. When the power delivered by the PV array reaches the power demand (6:30), the PEMFC generator is shut down and the PV generator takes charge of the power requirement. During the daylight period, the excess of power produced by the PV array is used to produce hydrogen from water electrolysis. Hydrogen is stored in a metal-hydride tank to be used for feeding the PEMFC generator when the PV generator cannot reach the power demand (especially, during the night). In the afternoon, when the power delivered by the PV becomes lower than the power demand (17:30) the PEMFC generator starts up again to cover the user load (17:30–24:00).

2.2. PEMFC model

This section deals with the dynamic nonlinear model of a PEMFC dedicated to nonlinear model-based control approaches. This is based on a set of generalized empirical equations developed for a basic model that could describe several types of fuel cells [10,13–15]. In order to simplify the analysis, several assumptions are made and are listed below.

- All gases are modeled as ideal gases.
- The total pressure inside the stack is uniform.
- Gas streams are saturated with vapor.
- Pure hydrogen is supplied to the anode.
- The air, that fed the cathode, is a mixture of nitrogen and oxygen by a ratio of 21:79.
- The electrolyte is fully saturated with water.
- The stack is well designed in such a way cells perform similarly and can be lumped as a stack.
- The temperature is homogeneous throughout the stack.
- Gases enthalpy variations are negligible.

2.2.1. Output voltage fuel cell modeling

The behavior of a fuel cell is strongly nonlinear and depends on several factors such as the current density, the fuel cell temperature and the partial pressure of reactants. The output voltage of a single fuel cell (V_{cell}) depends on the thermodynamic potential (E_{Nernst}), the ohmic drop (η_{ohm}) and the activation overvoltage (η_{act}). In the present approach, the concentration overvoltage links to gas access control is already incorporated in activation overvoltage.

$$V_{cell} = E_{Nernst} + \eta_{act} + \eta_{ohm} \quad (1)$$

The thermodynamic potential, also called Nernst voltage is obtained at the open-circuit condition under thermodynamic balance [15]

$$E_{Nernst} = 1.229 - 8.5 \times 10^{-4}(T - 298.15) + \frac{RT}{2F} \ln\left[P_{H_2}(P_{O_2})^{0.5}\right] \quad (2)$$

where T is the fuel cell temperature, P_{H_2} the partial pressure of hydrogen and P_{O_2} the partial pressure of oxygen. The ohmic overvoltage is written as a function of the temperature of the fuel cell, the cell electrode area (A_{fc}), the membrane thickness (l_m) and the current (I) [14].

$$\eta_{ohm} = -\frac{181.6I[1 + 0.03(I/A_{fc}) + 0.062(T/303)^2(I/A_{fc})^{2.5}]l_m}{A_{fc}[11.866 - 3(I/A_{fc})]\exp[4.18((T - 303)/T)]} \quad (3)$$

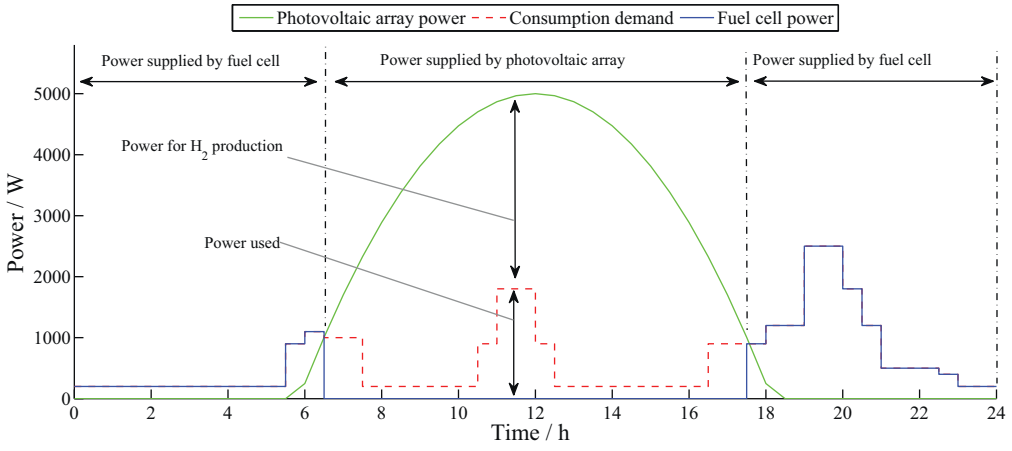

Fig. 2. Electric power produced by the PV arrays in summer (—) and a hypothetical charge profile for a residential household in La Reunion Island.

The effects of double layer capacitance charging at the electrode–electrolyte interface are described by considering the activation overvoltage dynamic [13].

$$\frac{dV_{act}}{dt} = \frac{I}{C_{dl}} - \frac{V_{act}}{R_{act}C_{dl}} \tag{4}$$

where C_{dl} is the double layer capacitance, $R_{act} = -\eta_{act}/I$ the activation resistance. η_{act} the activation overvoltage is empirically modeled using the following expression [14]:

$$\eta_{act} = \xi_1 + \xi_2 T + \xi_3 T \ \ln(C_{O_2}) + \xi_4 T \ln(I) \tag{5}$$

where

$$\xi_2 = 0.00286 + 0.0002 \ \ln(A_{fc}) + 4.3 \times 10^{-5} \ln(C_{H_2}) \tag{6}$$

ξ_1, ξ_3 and ξ_4 are constant parametric coefficients given in Table 1. The oxygen and hydrogen concentrations at the electrode/membrane interfaces are given using a Henry's law equation [15].

$$C_{O_2} = 1.97 \times 10^{-7} P_{O_2} \ \exp\left(\frac{498}{T}\right) \tag{7}$$

$$C_{H_2} = 9.174 \times 10^{-7} P_{H_2} \ \exp\left(\frac{-77}{T}\right) \tag{8}$$

Finally, the output voltage of a stack (V_{stack}) constitutes of N_{cell} cells in series are given by

$$V_{stack} = V_{cell} N_{cell} \tag{9}$$

2.2.2. Mass balance

According to the ideal gas law and the conservation rule, the variation of the partial pressure of each gas depends on the gas inlet flow rate, the gas consumption and the gas outlet flow rate. Thus, the dynamic of the partial pressure of hydrogen (P_{H_2}) at the anode and of the partial pressure of oxygen (P_{O_2}) at the cathode are given by

$$\frac{d}{dt}\left(\frac{P_{H_2} V_{an}}{RT}\right) = \dot{m}_{H_2,in} - \dot{m}_{H_2,out} - \dot{m}_{H_2,reacted} \tag{10}$$

$$\frac{d}{dt}\left(\frac{P_{O_2} V_{ca}}{RT}\right) = \dot{m}_{O_2,in} - \dot{m}_{O_2,out} - \dot{m}_{O_2,reacted} \tag{11}$$

where $\dot{m}_{H_2,in}$ and $\dot{m}_{O_2,in}$ are the inlet molar flow rate of hydrogen and oxygen, respectively, $\dot{m}_{H_2,reacted}$ and $\dot{m}_{O_2,reacted}$ the reacted molar flow rate of hydrogen and oxygen, respectively. Hydrogen and oxygen molar outlet flow rates can be estimated by the difference between partial pressure inside the stack and downstream pressure using the following equations [13]:

$$\dot{m}_{H_2,out} = k_{an}(P_{H_2} - P_{H_2}^{in}) \tag{12}$$

$$\dot{m}_{O_2,out} = k_{ca}(P_{O_2} - P_{O_2}^{out}) \tag{13}$$

The excess hydrogen is recirculated to the anode. The reacted gas flow rate is calculated by the Faraday's law (Eqs. (14) and (15)).

$$\dot{m}_{H_2,reacted} = N_{cell}\frac{I}{2F} \tag{14}$$

$$\dot{m}_{O_2,reacted} = N_{cell}\frac{I}{4F} \tag{15}$$

2.2.3. Energy balance

The energy balance of a PEMFC is a function of the total power ($\dot{E}_{tot}$) from the electrochemical reaction, the electrical power consumed by the electrical load ($\dot{E}_{elec}$), the heat flux both dissipated to the surroundings ($\dot{E}_{loss}$) and removed by the heat exchanger ($\dot{E}_{cool}$)

$$C_t \frac{dT}{dt} = \dot{E}_{tot} - \dot{E}_{elec} - \dot{E}_{loss} - \dot{E}_{cool} \tag{16}$$

The total power delivered is directly related to the reacted hydrogen molar flow rate and the enthalpy of reaction.

$$\dot{E}_{tot} = \dot{m}_{H_2,reacted}\Delta H \tag{17}$$

The power consumed by the electrical load and the heat flux dissipated at the stack surface are given by

$$\dot{E}_{elec} = V_{stack} I \tag{18}$$

$$\dot{E}_{loss} = h_{amb} S (T - T_{amb}) \tag{19}$$

where T_{amb} is the ambient temperature, h_{amb} the convective heat transfer coefficient and S the external stack surface. Finally, the heat flux removed by the coolant is obtained using a nonlinear model of the heat exchanger system [16].

$$\dot{E}_{cool} = (h_{cond} + h_{conv} I)\frac{(T - T_{c,in}) - (T - T_{c,out})}{\ln((T - T_{c,in})/(T - T_{c,out}))} \tag{20}$$

where $T_{c,in}$ and $T_{c,out}$ are the input and output water temperature, respectively. h_{cond} and h_{conv} are parameters which characterize the conduction and convection properties of the heat exchangers. $T_{c,out}$ is given as a function of the water mass flow rate ($\dot{m}_{cw}$), the water heat capacity (C_{pw}), the water volume (V_w), the water density (ρ_w) and the overall heat transfer coefficient (U_a).

$$\rho_w V_w C_{pw} \frac{dT_{c,out}}{dt} = \dot{m}_{cw} C_{pw}(T_{c,in} - T_{c,out}) + U_a\left(T - \frac{T_{c,in} + T_{c,out}}{2}\right) \tag{21}$$

All parameters values and description are gathered in Table 1.

3. Control design

In this study, the PEMFC generator is a part of the stand-alone hybrid system and used to cover the energy demand when the PV generator is deficient. Consequently, the first controlled variable is the output power of the PEMFC system. To ensure the reliability of the stand-alone hybrid system, the output power of the PEMFC generator has to track changes in setpoint with accuracy and short time response even when extreme load changes are imposed. To reach these control objectives, the choice of the manipulated variable and the controller are crucial. In this study, the control of the output power is based on a nonlinear model-based predictive control (NMPC) with the molar flow rate of hydrogen as manipulated variable. Several authors report the robustness and efficiency of the NMPC when dealing with fuel cell control [9,10,17].

It is well-known that the performance and the reliability of the PEMFC system strongly depend on its operating temperature. Therefore, to ensure optimal operating condition and avoid any risk of damage due to high temperature, the control of the PEMFC temperature is mandatory. In this study, the control of this second controlled variable is based on a global linearizing control (GLC) approach using the mass flow rate of water as manipulated variable. Differential geometry has been accepted as a relevant tool for the design of nonlinear controllers and has proved its efficiency for numerous nonlinear chemical processes. Most of approaches concerned with this tool consist in a feedback linearization, either input–output or input-state [18–21]. Regarding the GLC, an input–output linearizing technique, the nonlinear control law is based directly on the nonlinear model of the PEMFC system. According to on-line objective applications, GLC appears as a suitable alternative to the widely used NMPC to reduce the computation time of the control variable.

In short, the control of the output power is performed using an NMPC strategy whereas the control of the PEMFC temperature is based on a GLC algorithm. The benefit of the proposed control strategy (NMPC + GLC) in terms of computation time efficiency is studied

Table 1
Parameter values for the Ballard MK5-E PEMFC 5 kW system [13].

Symbol	Description	Value	Unit
N_{cell}	Number of cell	35	
A_{fc}	Cell electrode area	232	cm^2
ξ_1	Parametric coefficient	−0.948	
ξ_3	Parametric coefficient	7.6×10^{-5}	
ξ_4	Parametric coefficient	-1.93×10^{-4}	
C_{dl}	Double layer capacitance	8.12	F
V_{an}	Anode volume	0.005	m^3
V_{ca}	Cathode volume	0.01	m^3
k_{an}	Flow constant at the anode	0.065	$mol\,s^{-1}\,atm^{-1}$
k_{ca}	Flow constant at the cathode	0.065	$mol\,s^{-1}\,atm^{-1}$
$P^{in}_{H_2}$	Hydrogen pressure at the inlet	3	atm
$P^{out}_{O_2}$	Oxygen pressure at the outlet	3	atm
$\dot{m}_{O_2,in}$	Oxygen inlet flow rate	2	$mol\,s^{-1}$
l_m	Membrane thickness	178×10^{-4}	cm
$h_{amb}S$	Stack heat transfer coefficient	17	$W\,K^{-1}$
T_{amb}	Ambient temperature	298	K
$T_{c,in}$	Cooling water inlet temperature	298	K
ΔH	Hydrogen consumption enthalpy	285.5	$kJ\,mol^{-1}$
C_t	Thermal capacitance	17.9	$kJ\,K^{-1}$
h_{cond}	Heat exchanger conductive index	35.55	$W\,K^{-1}$
h_{conv}	Heat exchanger convective index	0.025	$W\,K^{-1}\,A^{-1}$
C_{pw}	Heat capacity of water	4.184	$kJ\,kg^{-1}\,K^{-1}$
ρ_w	Water density	1000	$kg\,m^{-3}$
V_w	Water volume	2.5×10^{-3}	m^3
U_a	Overall heat transfer coefficient	241	$W\,K^{-1}$

in Section 4. With this aim, a comparison between the proposed strategy and a classical multivariable NMPC strategy is performed.

3.1. NMPC of output fuel cell power

The NMPC is based on a prediction of the future output of the system to calculate the current control action. In practice, the current control action is obtained by solving on-line an optimization problem. The aim of the optimization problem is to find the optimal solution of a nonlinear cost function that minimizing the mean squared difference between predicted outputs and target values. This strategy offers a great flexibility and robustness. In fact, the optimization problem can handle penalty for variations in the control variable (e.g. to avoid excessive variation), degree of importance of the setpoint tracking accuracy, the error modeling, etc. In this study, the optimization problem can be rewritten as

$$\min_{u(k/k),u(k+1/k),\ldots,u(k+N_u/k)} J(k) = \min_{u(k/k),u(k+1/k),\ldots,u(k+N_u/k)} \times \left(\sum_{i=N_1}^{Ny} \gamma(e(k+i/k))^2 + \sum_{i=1}^{Nu} \beta \Delta u^2(k+i/k) \right) \quad (22)$$

subject to constraints on the manipulated variable

$$u_{\min} \le u(k+i/k) \le u_{\max} \quad \text{for} \quad i = 1, 2, \ldots, N_u \quad (23)$$

where $u(k)$, the control variable, is the molar flow rate of hydrogen at time k, N_y and N_u the predictive and control horizon, respectively, γ and β two weighting parameters. The prediction horizon corresponds to the future time interval used to compute the process output predictions with the PEMFC model. The control horizon corresponds to the time interval when present and future control actions are computed. The optimization parameter N_1 determines, together with the prediction horizon the coincidence horizon. The trajectory tracking error and the changes in the control variable are formulated by

$$e(k+i/k) = y_{sr}(k+i/k) - (y_m(k+i/k) + y(k) - y_m(k)) \quad (24)$$

$$\Delta u(k+i/k) = u(k+i/k) - u(k+i-1/k) \quad (25)$$

where y_{sr} is the target value and y_m the model output. y_{sr} allows to take into account the dynamic of the system, it gives the trajectory to follow to make the process output reach the setpoint w. Fig. 3 illustrates the overall NMPC principle.

3.2. GLC of fuel cell temperature

The objective of input–output linearization is to obtain a nonlinear control law directly based on the nonlinear model of the system. To understand the GLC approach proposed in this paper, a brief recall about the concept of differential geometry is essential. For brevity, it will be limited to single-input single-output (SISO) system. However, the idea can be straightforwardly extended to a MIMO system. Considering the nonlinear SISO system given by

$$\dot{x}(t) = f(x) + g(x)u \quad (26)$$

$$y(x) = h(x(t)) \quad (27)$$

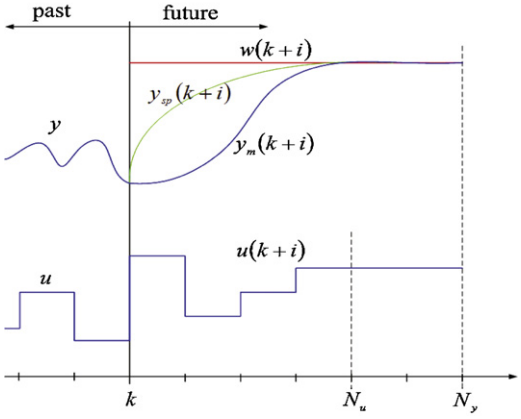

Fig. 3. NMPC principle.

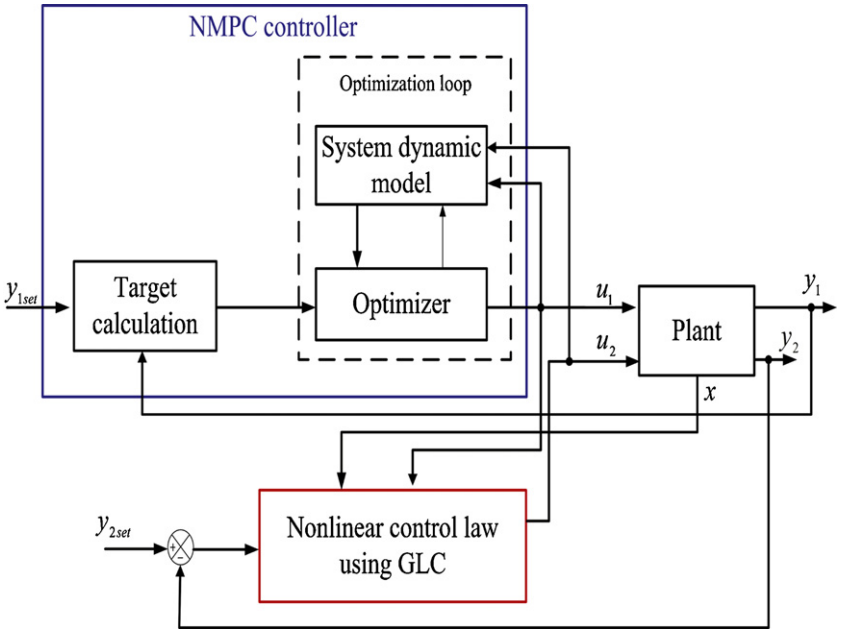

Fig. 4. Overall control scheme of the PEMFC system, where y_{1set} and y_{2set} are the output power setpoint and the temperature stack setpoint, respectively.

where $x \in R^n$ is the state vector, u the input vector and y the output vector. An input–output relation can be deduced

$$y^r(t) = L_f^r h(x(t)) + L_g(L_g^{r-1} h(x(t)))u(t) \tag{28}$$

where $y^r(t) = d^r y/dt^r$, $L_f^r h$ and $L_g^r h$ are the rth Lie derivatives of $h(x(t))$ along f and g. $r \leq n$ is the relative degree of the system, i.e. the number of times the output has to be differentiated with respect to time before one input u appears explicitly in the resulting equations.

Once this relation is established, a closed-loop control can be designed. In most process control applications, to reduce the effect of unmeasured disturbances and plant/model mismatch, the control law includes an integral term [18,22,23]. Consequently, considering a setpoint to track, denoted y_{sp}, the tracking problem is given by

$$y^r(t) = y_{sp}^r + \sum_{i=0}^{r-1} k_i \Re^{(i)}(t) + \alpha_0 \int_{\tau_0}^{\tau} \Re(t) d\tau \tag{29}$$

where $\Re(t) = y_{sp}(t) - y(t)$ is the pursuit error, $\Re^{(i)} = d^i \Re/dt^i$, $k_0, k_1, \ldots, k_{r-1}$ and α_0 the controller tuning parameters. Finally, the control law is deduced from Eqs. (28) and (29)

$$u(t) = \frac{y_{sp}^r + \sum_{i=0}^{r-1} k_i \Re^{(i)}(t) + \alpha_0 \int_{\tau_0}^{\tau} \Re(t) d\tau - L_f^r h(x(t))}{L_g(L_g^{r-1} h(x(t)))} \tag{30}$$

In this study, according to the dynamic nonlinear model of the PEMFC system, the GLC approach is used to control the temperature of the PEMFC with the water mass flow rate as control variable.

3.3. Control of the PEMFC system

The control of the PEMFC system is based on a NMPC of the output power (y_1) using the hydrogen molar flow rate (u_1) as control variable and on a GLC strategy to regulate the PEMFC temperature (y_2) by manipulated the water mass flow rate (u_2). Widely known and used for its convergence and robustness properties, the Levenberg–Marquard's algorithm is used here to solve on-line the optimization problem of the NMPC strategy. The overall control scheme of the MIMO PEMFC system is illustrated in Fig. 4.

Due to physical constraints, the water mass flow rate range from 0.3 to 0.12 kg s^{-1} and the hydrogen molar flow rate range from 0 to 1 mol s^{-1}.

4. Simulation results

In order to evaluate the performance of the proposed control scheme, a 5 kW PEMFC plant system is simulated in the Matlab™ environment. It should be pointed out that an operating fuel cell plant requires the regulation of other variables, to avoid for instance oxygen starvation or membrane flooding or dehydration. In the following simulations, it is assumed these variables have already been well controlled.

4.1. Control performance

The performance of the proposed control strategy, in terms of setpoint tracking, disturbances rejection and robustness against model mismatch in presence of noise measurement, is studied via three control scenarios. The first scenario evaluates the performance of the proposed strategy when large step changes of load power demand appear. The second one allows us to study the proposed strategy when a step temperature is set. Finally, to evaluate the robustness of the controller, the third scenario considers a model mismatch in parameters. In this purpose, the flow constant at the anode (k_{an}) and the overall heat transfer coefficient (U) are randomly increased and decreased from their nominal values by 20% every 10 min. Moreover, to be closer to the experimental conditions a white Gaussian noise with a signal to noise ratio of 1% is added to the process outputs simulator.

Fig. 5 shows results for the first scenario. A good performance in PEMFC output power setpoint tracking and a satisfactory regulation of the stack temperature in presence of power disturbances are established. Moreover, the dynamic of both manipulated variables is entirely suitable. This first scenario highlights the requirement of an appropriate control of the stack temperature to avoid any damage of the PEMFC.

Fig. 6 shows a correct running of the proposed strategy in temperature setpoint tracking, considering a step change of fifteen degrees, and an excellent regulation of the output power in

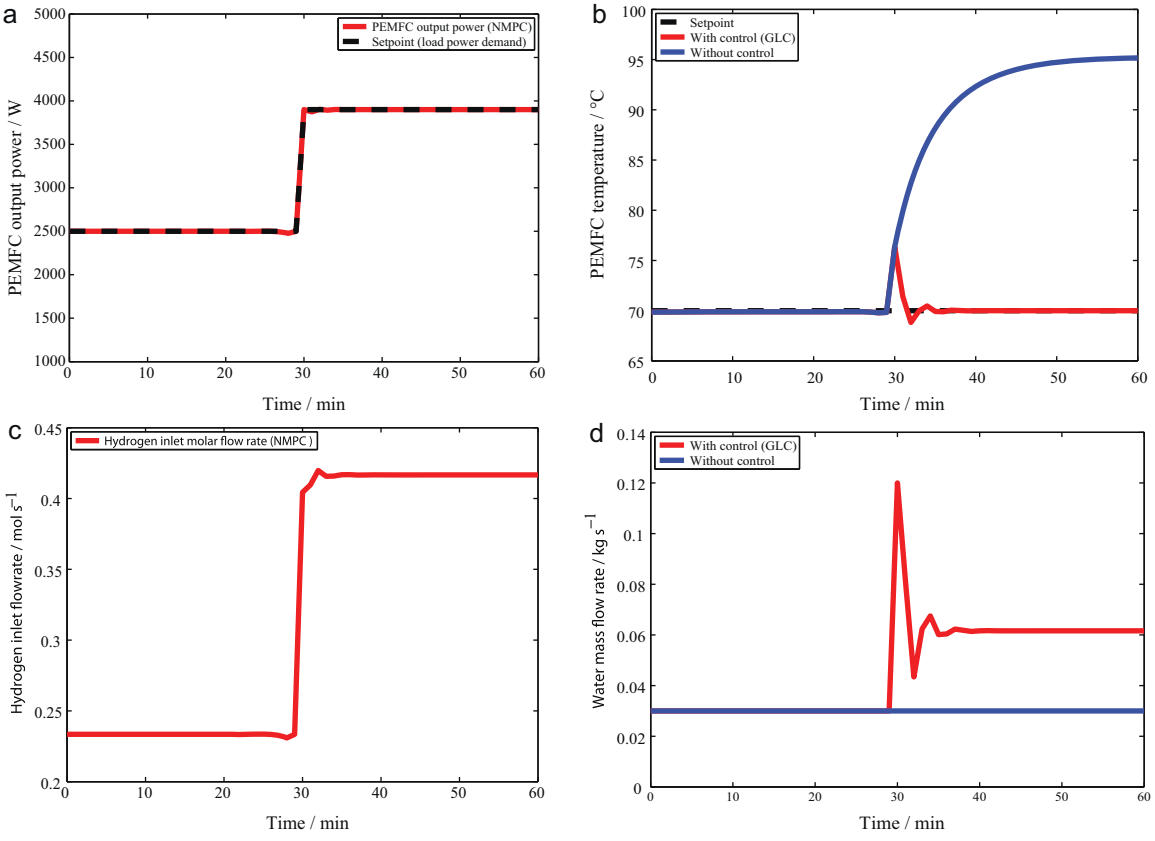

Fig. 5. First control scenario: (a) PEMFC output power; (b) stack temperature; (c) hydrogen molar flow rate; (d) water mass flow rate.

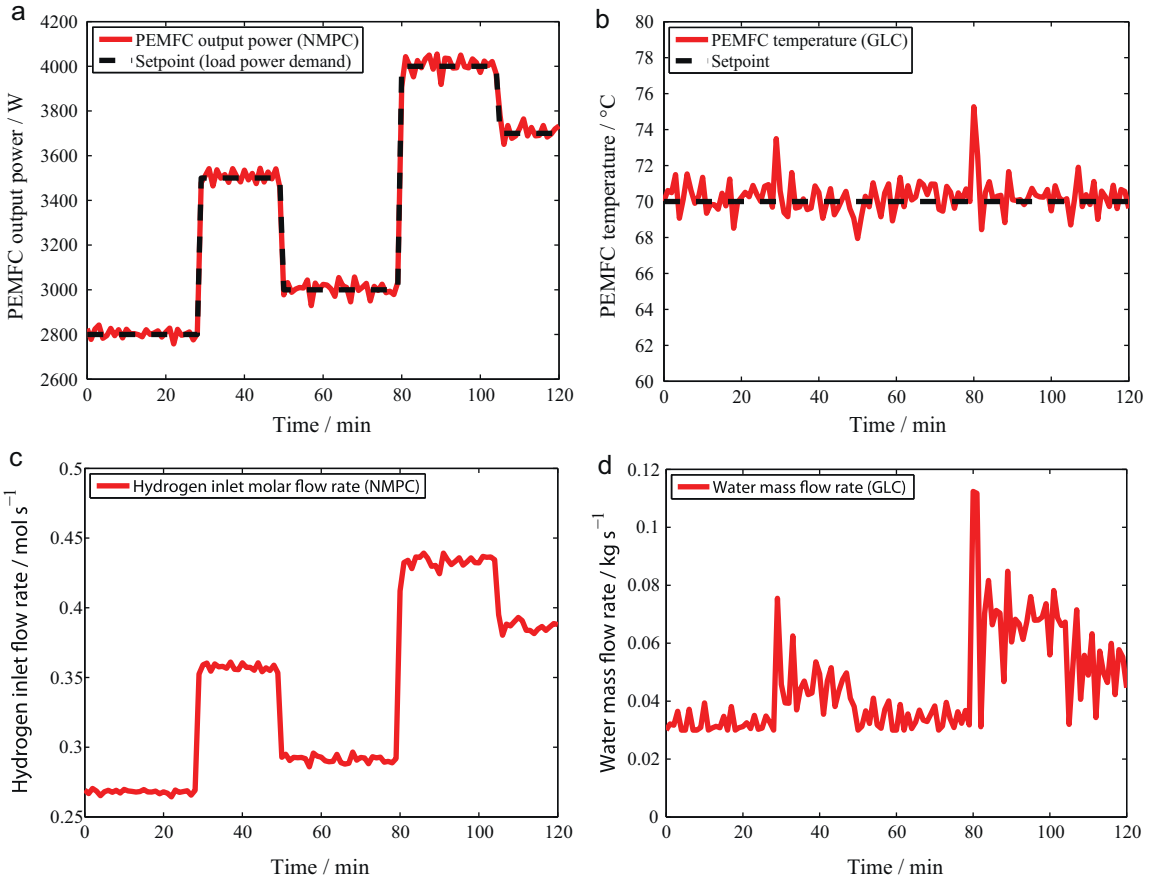

Fig. 6. Second control scenario: (a) PEMFC output power; (b) stack temperature; (c) hydrogen molar flow rate; (d) water mass flow rate.

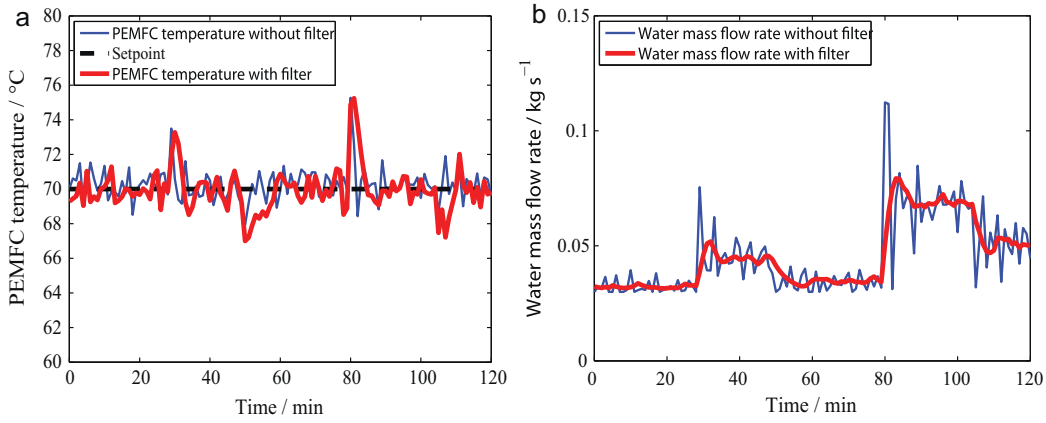

Fig. 7. Third control scenario: (a) PEMFC output power; (b) stack temperature; (c) hydrogen molar flow rate; (d) water mass flow rate.

presence of temperature disturbances. The saturation observed in Fig. 6d between 28 and 33 min is due to previously mentioned physical constraints on water mass flow rate. This second scenario confirms that the performance of the PEMFC strongly depends on its operating temperature. In one hand, too lower temperature slows down mass and charge transfer reducing the PEMFC performance. In the other hand, too higher temperature could damage the PEMFC and impacts its performance.

Fig. 7 demonstrates the control effectiveness of the multivariable proposed control strategy under several step changes of high load power demand in presence of high level of noise measurement and plant/model mismatch. The excellent accuracy in power setpoint tracking and the satisfactory regulation of the stack temperature emphasize the robustness of the proposed controller against unavoidable plant/model mismatch and noise measurement.

However, whereas the manipulated variable computed by the NMPC controller is smooth, it can be pointed out that the water flow rate calculated using GLC is affected by the noise. In the case of GLC, since the control law is directly deduced from the model process, the manipulated variable is affected by the noise measurement. In practice, this limitation is easily overcome either filtering on-line the measurements or directly the control action. A widely used heuristic rule consists of applying a first-order filter to the control action to reduce high frequency oscillation. In this manner, the filtered control action $u_2^{filtered}$ is obtained using the relation (31):

$$u_2^{filtered}(t) = \alpha u_2^{filtered}(t-1) + (1-\alpha)u_2^{GLC}(t) \quad (31)$$

where $u_2^{GLC}(t)$ is the control action calculated by the GLC approach and α the filter coefficient between 0 and 1.

However, when dealing with optimal control, this approach leads to a sub-optimal solution of the control action, which in some cases could involve a significant decrease of the setpoint tracking accuracy.

In the present case, an appropriate setting of the filter parameter allows to smooth the control action without decreasing the setpoint tracking performance. Considering a filtering parameter α equal to 0.5, Fig. 8 illustrates the benefits of this heuristic rule to significantly reduce the oscillation of the control variable in presence of noise measurement and plant/model mismatch (third scenario configuration).

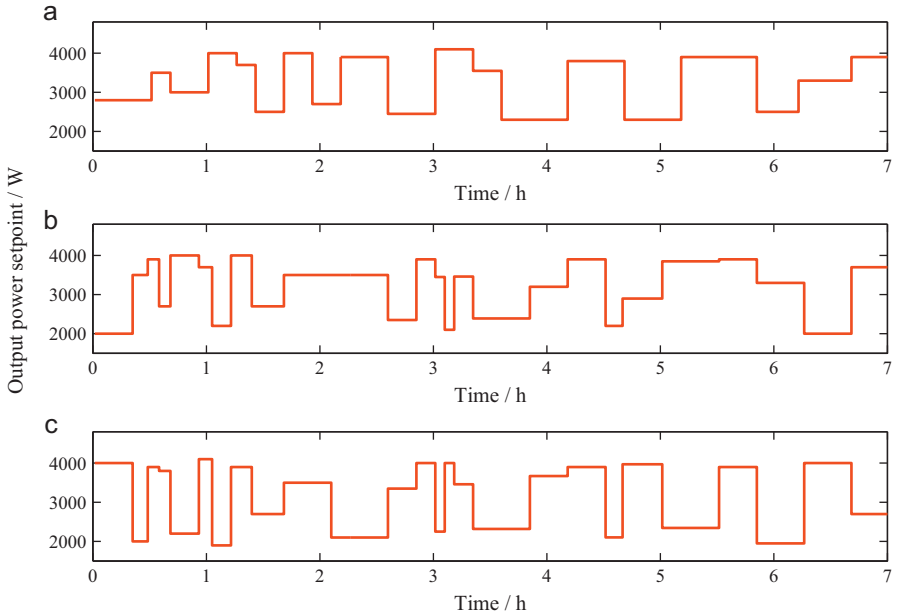

Fig. 8. Filtering approach performance: (a) stack temperature; (b) water mass flow rate.

Table 2
Comparison between proposed control strategy and classical NMPC strategy in terms of accuracy and computational time.

	Classical strategy	Proposed strategy
Profile 1		
RMSE for power	0.468	0.329
RMSE for temperature	0.253	0.176
MCT (s)	20.028	4.76
Profile 2		
RMSE for power	0.812	0.687
RMSE for temperature	0.274	0.218
MCT (s)	18.479	5.080
Profile 3		
RMSE for power	0.787	0.712
RMSE for temperature	0.365	0.318
MCT (s)	21.374	5.728

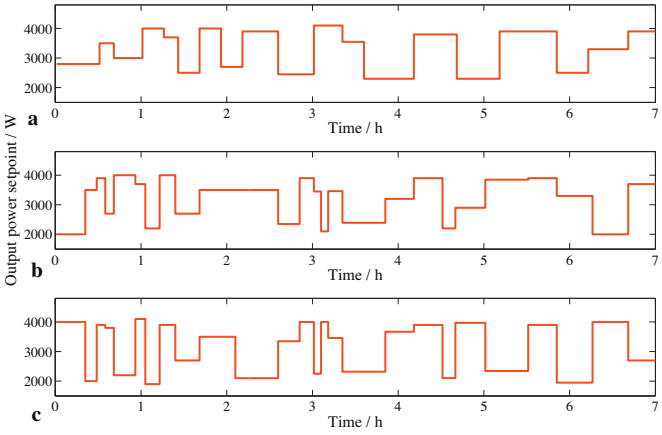

Fig. 9. Power demand profile: (a) profile 1; (b) profile 2; (c) profile 3.

4.2. Computational time efficiency

In order to highlight the benefit due to reduction of computational time, classical multivariable NMPC strategy has been compared to the proposed control strategy (NMPC + GLC). Therefore, a classical multivariable NMPC strategy is implemented in Matlab® environment considering the water mass flow rate and the hydrogen molar flow rate as manipulated variables, and the output power and the stack temperature as controlled variables. The performance of each strategy, in terms of computational time efficiency, is evaluated on three typical power demand profiles (Fig. 9), considering a constant setpoint of 70 °C for the stack temperature.

Table 2 summarizes the computational time efficiency and the setpoint tracking accuracy of each strategy. This study proposes simulations, using Matlab® software and running with 2-GHz and 32-bit computer. The root mean square error (RMSE) criterion is used to evaluate the performance in terms of setpoint tracking accuracy, whereas the computational time efficiency is investigated using the mean computational time (MCT):

$$\mathrm{RMSE} = \frac{\sqrt{\sum_{i=1}^{n}(y_{sp\ i} - y_i)^2}}{n} \tag{32}$$

$$\mathrm{MCT} = \frac{\sum_{i=1}^{n} \mathrm{CT}_i}{n} \tag{33}$$

where n is the number of data and CT_i the time required to solve the control problem at time $t = i$.

It can be noticed that for similar accuracies of RMSE, the combination of NMPC and GLC algorithms is four times faster than a classical multivariable NMPC strategy. Regarding on-line application objectives, the proposed control strategy appears to be a suitable alternative to the classical multivariable NMPC controller.

5. Conclusions

In this work, an innovative model-based control approach of a proton exchange membrane fuel cell is proposed. In this aim, a MIMO dynamic nonlinear model of a PEMFC, dedicated to nonlinear model-based control approaches, is developed and implemented in Matlab™. To control the output power and the stack temperature, a nonlinear model-based predictive control strategy (NMPC) and a global linearizing control (GLC) approach are designed, directly based on this model.

The simulation results, for a 5 kW PEMFC power plant, demonstrated that the proposed control strategy led to good performance in setpoint tracking, disturbances rejection and robustness against plant/model mismatch and noise. Regarding on-line application objective, the proposed strategy appears to be four times faster than classical multivariable NMPC strategies. It is well-known that the cell performance changes along its life, the model parameters have to be adjusted to reduce plant/model mismatch. Therefore, semi-empirical PEMFC model used by this control approach makes easy the tuning of the model parameters in order to reduce plant/model mismatch during lifetime of cell. The tuning of the model parameter could be performed off-line through experiments, or on-line using an optimization algorithm.

This proposed model-based control approach appears suitable to be included in the overall control scheme of the stand-alone hybrid power generation system used to cover the daily power consumption of a typical household in subtropical island (Ile de La Réunion: 21° 6′ S/55° 36′ E).

Acknowledgments

The authors would like to kindly acknowledge Pr. Jean-Daniel Lan-Sun-Luk for the fruitful scientific discussions. M. Patrick Jeanty for the solar experimental data.

References

[1] S. Krauter, R. Araujo, Proceedings of the 16th European Photovoltaic Solar Energy Conference, Glasgow, UK, 2000, James & James, London, 2000, pp. 2575–2577.
[2] P. Hollmuller, J. Joubert, B. Lachal, K. Yvon, Int. J. Hydrogen Energy 25 (2000) 97–109.
[3] J.J. Hwang, W.R. Chang, A. Su, Int. J. Hydrogen Energy 33 (2008) 3801–3807.
[4] J.J. Hwang, L.K. Lai, W. Wu, W.R. Chang, Int. J. Hydrogen Energy 34 (2009) 9531–9542.
[5] P.L. Zervas, H. Sarimveis, J.A. Palyvos, N.C.G. Markatos, J. Power Sources 181 (2008) 327–338.
[6] S.R. Huang, C.Y. Lin, C.C. Wu, S.J. Yang, Int. J. Hydrogen Energy 33 (2008) 5205–5217.
[7] F.C. Wang, C.C. Ko, Int. J. Hydrogen Energy 35 (2010) 10437–10445.
[8] R.N. Methekar, V. Prasad, R.D. Gudi, J. Power Sources 165 (2007) 152–170.
[9] X.W. Zhang, S.H. Chan, H.K. Ho, J. Li, G. Li, F. Zhenping, Int. J. Hydrogen Energy 33 (2008) 2355–2366.
[10] W. Wu, J.P. Xu, J.J. Hwang, Int. J. Hydrogen Energy 34 (2009) 3953–3964.
[11] Q. Li, W. Chen, Y. Wang, J. Jia, M. Han, J. Power Sources 194 (2009) 338–348.
[12] B. Shabani, J. Andrews, Int. J. Hydrogen Energy 36 (2011) 5442–5452.
[13] M.J. Khan, M.T. Iqbal, Fuel Cells 5 (2005) 463–475.
[14] R.F. Mann, J.C. Amphlett, M.A.I. Hooper, H.M. Jensen, B.A. Peppley, P.R. Roberge, J. Power Sources 86 (2000) 173–180.
[15] J.C. Amphlett, R.M. Baumert, R.F. Mann, B.A. Peppley, P.R. Roberge, J. Electrochem. Soc. 142 (1995) 1–8.
[16] J.R. Macdonald, Impedance Spectroscopy – Emphasizing Solid Materials and Systems, John Wiley & Sons Inc., New York, 1987.
[17] J. Golbert, D.R. Lewin, J. Power Sources 135 (2004) 135–151.
[18] J. Madar, J. Abonyi, F. Szeifert, Eng. Appl. Artif. Intell. 18 (2005) 335–343.
[19] J. Gonzalez, R. Aguilar, J. Alvarez-Ramirez, G. Fernandez, M. Barron, Artif. Intell. Eng. 13 (1999) 405–412.
[20] H. Nijmeijer, A.J. Van der Schaft, Nonlinear Dynamical Control System, Springer, Berlin, 1990.
[21] J.J. Slotine, W. Li, Applied Nonlinear Control, Prentice Hall, New Jersey, 1991.
[22] R. Dunia, T. Edgar, B. Fernandez, Chem. Eng. Sci. 52 (1997) 2205–2222.
[23] M. Duvall, B.J. Riggs, P. Lee, Control Eng. Pract. 9 (2001) 471–481.